Available online at www.sciencedirect.com

SCIENCE DIRECT®

Journal of Colloid and Interface Science 291 (2005) 75–83

Journal of Colloid and Interface Science

www.elsevier.com/locate/jcis

Adsorption and conformation of carboxymethyl cellulose at solid–liquid interfaces using spectroscopic, AFM and allied techniques

Jing Wang, P. Somasundaran [*]

NSF Industry/University Cooperative Research Center for Advanced Studies in Novel Surfactants, Columbia University, New York, NY, 10027, USA

Received 22 February 2005; accepted 28 April 2005

Abstract

Carboxymethyl cellulose (CMC) is a polysaccharide which is widely used in many industrial sectors including food, textiles, paper, adhesives, paints, pharmaceutics, cosmetics and mineral processing. It is a natural organic polymer that is non-toxic and biodegradable. These properties make it ideal for industrial applications. However, a general lack of understanding of the interaction mechanism between the polysaccharides and solid surfaces has hindered the application of this polymer. In this work, adsorption of CMC at the solid–liquid interface is investigated using adsorption and electrophoretic mobility measurements, FTIR, fluorescence spectroscopy, AFM and molecular modeling. CMC adsorption on talc was found to be affected significantly by changes in solution conditions such as pH and ionic strength, which indicates the important role of electrostatic force in adsorption. The pH effect on adsorption was further proven by AFM imaging. Electrokinetic studies showed that the adsorption of CMC on talc changed its isoelectric point. Further, molecular modeling suggests a helical structure of CMC in solution while it is found to adsorb flat on the solid surface to allow its OH groups to be in contact with the surface. Fluorescence spectroscopy studies conducted to investigate the role of hydrophobic bonding using pyrene probe showed no evidence of the formation of hydrophobic domains at talc–aqueous interface. Urea, a hydrogen bond breaker, markedly reduced the adsorption of CMC on talc, supports hydrogen bonding as an important factor. In FTIR study, the changes to the infrared bands, associated with the C–O stretch coupled to the C–C stretch and O–H deformation, were significant and this further supports the strong hydrogen bonding of CMC to the solid surface. In addition, Langmuir modeling of the adsorption isotherm suggests hydrogen bonding to be a dominant force for polysaccharide adsorption since the adsorption free energy of this polymer was close to that for hydrogen bond formation. All of the above results suggest that the main driving forces for CMC adsorption on talc are a combination of electrostatic interaction and hydrogen bonding rather than hydrophobic force.

Keywords: Talc; CMC; Polymer adsorption; Fluorescence; AFM; Model; Zeta potential; FTIR

1. Introduction

Talc is a layered hydrous magnesium silicate in which the layers are held together by van der Waals bonds. During grinding, two different types of surfaces are formed. Basal cleavage planes are formed by the rupture of van der Waals bonds, and because the resulting planes contain no broken Si–O and Mg–O bonds, the surface is neutral and hydrophobic. However, the edges of the mineral sheets contain broken Si–O and Mg–O bonds and, consequently, are charged sites exhibiting hydrophilic properties.

Carboxymethyl cellulose (CMC) is a natural anionic polysaccharide. The repeating unit of CMC is shown in Fig. 1. Each unit contains three OH groups and these groups are available for hydrogen bonding [1].

Carboxymethyl cellulose has been used in the flotation of cassiterite to depress calcite [2]. It has also been extensively tested in the flotation of sulphide ores to depress silicates [3–5]. In spite of a large number of studies conducted in the past, the mechanism of adsorption of CMC on solids is not yet well understood. Mackenzie [6], Pugh [7], Healy [8]

---

[*] Corresponding author.
E-mail address: ps24@columbia.edu (P. Somasundaran).

0021-9797/$ – see front matter © 2005 Elsevier Inc. All rights reserved.
doi:10.1016/j.jcis.2005.04.095

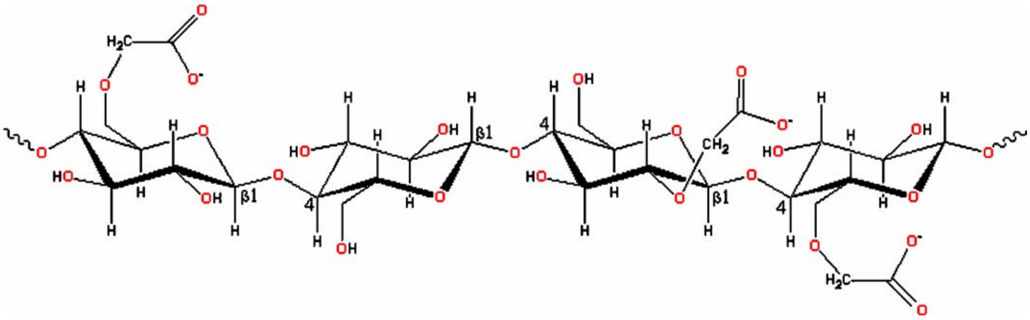

Fig. 1. The monomeric structure of CMC.

and Rath et al. [9,10] proposed that the mechanisms governing the adsorption of polymers on mineral surfaces include hydrophobic interaction, hydrogen bonding, chemical and electrostatic interactions. However, the reasons for the selectivity of its adsorption on minerals has not been accounted for. Steenberg et al. [11,12] and Ralston et al. [13] proposed that the adsorption of polysaccharide on talc occurs mainly at the basal planes via hydrophobic force. In contrast, Rath et al. [14] and Jucker et al. [15] proposed that the adsorption of polysaccharide occurs through hydrogen bonding on solids.

The objective of this study was to clarify the mechanistic aspects of the interactions between CMC and talc using a combination of spectroscopic, microscopic, molecular modeling, electrostatic and adsorption techniques.

2. Experimental

2.1. Materials

Talc sample of 40 µm size and BET surface area of 19.75 m^2/g was obtained from Cytec Industries. The composition analysis was done by Galbraith Laboratory, Inc. The samples were burned in a Schoniger flask and then the composition was read using an ionic electrode. The result indicated that it was a very pure sample with only 0.7% of tremolite ($Ca_2Mg_5Si_8O_{22}(OH)_2$). Mica in the form of flat plate purchased from Ted Pella, Inc., was also used in AFM studies.

Carboxymethyl cellulose, an anionic polysaccharide, was obtained from Cytec Industries. GPC analysis showed the average molecular weight of 714,900 and polydispersity of 4.59. All CMC stock solutions were prepared by quickly adding 0.045 g of CMC powder into 45 ml of vigorously stirred water and further stirring for 30 min. The solution was refrigerated overnight to ensure complete hydration or dissolution of CMC and then filtered through Whatman #4 to remove any undissolved impurities.

pH of the solutions and suspensions was adjusted using Fisher standard hydrochloric acid and sodium hydroxide solutions. Reagent grade potassium chloride from APACHE Chemicals, Inc., was used to adjust the ionic strength of solutions. 1-pyrene butyric acid and 1,3-dicyclohexyl carbodiimide (DCC) bought from Aldrich were used in the fluorescence probe labeling of the polymers. Urea (Fisher Chemical), phenol (EM Science) and 98% sulfuric acid (Amend Drug & Chemical Co., Inc.) were used for colorimetric experiments. The water used was triply distilled.

2.2. Experiments

2.2.1. Adsorption measurements

The suspensions of solids, with ionic strength adjusted using KCl and pH adjusted using HCl and KOH at 10% solid loading, were ultrasonicated for 30 min and then stirred magnetically for 2 h. CMC stock solution was then added to the solid suspension and left for conditioning overnight. The suspensions were then centrifuged and the supernatants pipetted out for determination of CMC concentration by a Total Organic Carbon Analyzer. The adsorption density of CMC on solid was calculated from the data for initial and residual CMC concentrations.

2.2.2. Colorimetric method

A colorimetric method described by Dubois et al. [16] was used in experiments wherein other organic additives, such as urea, were used. 0.05 ml 80% phenol and 5 ml 98% sulfuric acid were added to 2 ml of supernatant obtained after centrifugation and after 4 h of color development under warm conditions, absorbance was measured at a wavelength of 487.5 nm using SHIMADZU UV-1201 UV–vis spectrophotometer. Adsorption density of CMC on talc was calculated from the difference in absorbance.

2.2.3. Electrokinetic measurements

Small amounts of talc were added to desired amounts of 10^{-3} M KNO_3 solution and ultrasonicated for 30 min, magnetically stirred for 2 h and the pH adjusted using HCl or KOH. Finally, the CMC stock solution was added and left for conditioning for 16 h. The zeta potential was then measured using a Zeta meter.

2.2.4. FTIR study

The infrared spectra of talc, polysaccharides and polymer adsorbed talc were recorded using a Model FTS7000 series Fourier transform infrared spectrometer from Digilab operating in the range 4000–350 cm^{-1}. Approximately 2 mg of the desired powder sample was thoroughly mixed with 200 mg of spectroscopic grade KBr and pressed into pellets for recording the spectra.

2.2.5. *Fluorescence spectroscopy*

Suspensions of talc at 10% solid loading were ultrasonicated for 30 min and mixed for 2 h with a magnetic stirrer. Stock solution of pyrene-labeled CMC was then added to the talc suspension. The vials containing the suspensions were quickly wrapped with aluminum foil to keep the light away and left to condition overnight. Finally, the hydrophobicity of the supernatant and the solid were analyzed separately using a LS-1 fluorescence spectrophotometer (Photon Technology International).

2.2.6. *AFM analysis*

The atomic force microscopy (AFM) system used was Nanoscope III from Digital Instruments. The measurements were performed in air or underwater in tapping mode using a V-shaped Si_3N_4 cantilever covered with gold on the back for laser beam reflection. Two types of tips, MESP-10 and NP-20, were used in air and underwater, respectively. All images were collected in the height mode, which keeps the force constant.

2.2.7. *Molecular modeling*

Molecular modeling (Macromodel) is a powerful tool for exploring the conformation of polysaccharide in solvents. Macromodel was applied to study the conformation of CMC. Accelrys Material Studio was also used to explore the conformation of adsorbed polysaccharides on solid.

3. Results and discussion

3.1. *Molecular modeling*

Fig. 2 shows the computer simulated molecular space filling structure of CMC in both vacuum and aqueous environments. Each of them contains 5 repeat units. It is seen that polymer chains tend to be in a more stretched helical form in water than in vacuum. The complex helical structure shown in Fig. 3 is a piece of polymer chain containing 50 repeat units. It is clear that the OH groups tend to stick out of the helix. According to the simulation, there is no change in the structure when the number of repeat units is increased further from 50 to 100.

From computer simulation by Accelrys Material Studio (Fig. 4), we find the CMC molecules to choose a relatively flat conformation on talc surface to let more of its OH groups to be in contact with the surface.

3.2. *Electrokinetic studies*

It is evident from the electrokinetic data shown in Fig. 5 that the surface of talc is negatively charged and the isoelectric point (iep) is located around pH 2.5. Above pH 2.5, the electronegative character increases with increase in pH up to pH 4 and thereafter remains almost constant. CMC is in free acid form (neutral) at pH 3.5, and the acid groups are ionized (negatively charged) at about pH 7.0. The adsorption of CMC on talc caused a shift of iep from 2.5 to 3.25, which indicates the important role of electrostatic interaction in this system.

3.3. *Adsorption studies*

3.3.1. *Influence of pH*

Fig. 6 shows adsorption isotherms of CMC on talc at pH 3 and pH 9. It can be seen that the adsorption density of CMC is reduced with the increase of pH from 3 to 9. If electrostatic interaction has an important role in the adsorption process, the adsorption density of CMC on talc will be expected to be reduced significantly, and since CMC is more negatively charged at pH 9 than at pH 3 and the surface charge of talc does change from pH 3 to 9, it can be concluded that electrostatic repulsion plays an important role in this system.

3.3.2. *Influence of ionic strength*

Adsorption isotherms of CMC on talc at pH 9 at different ionic strengths are shown in Fig. 7. Adsorption density increases with increase of ionic strength, which can be attributed to the "screening" effect of salt. Since at pH 9, both the polymer and talc are negatively charged, the addition

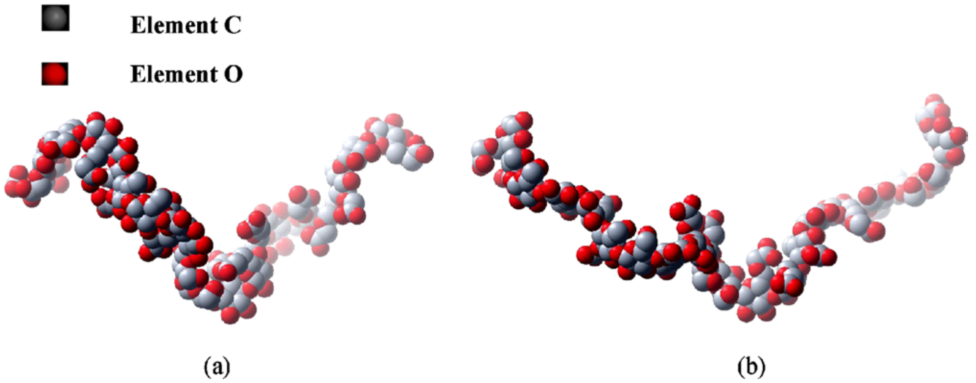

Fig. 2. Computer simulated molecular CPK (space filling) structure of CMC in: (a) no solvent, (b) aqueous environment (each contains five repeat units).

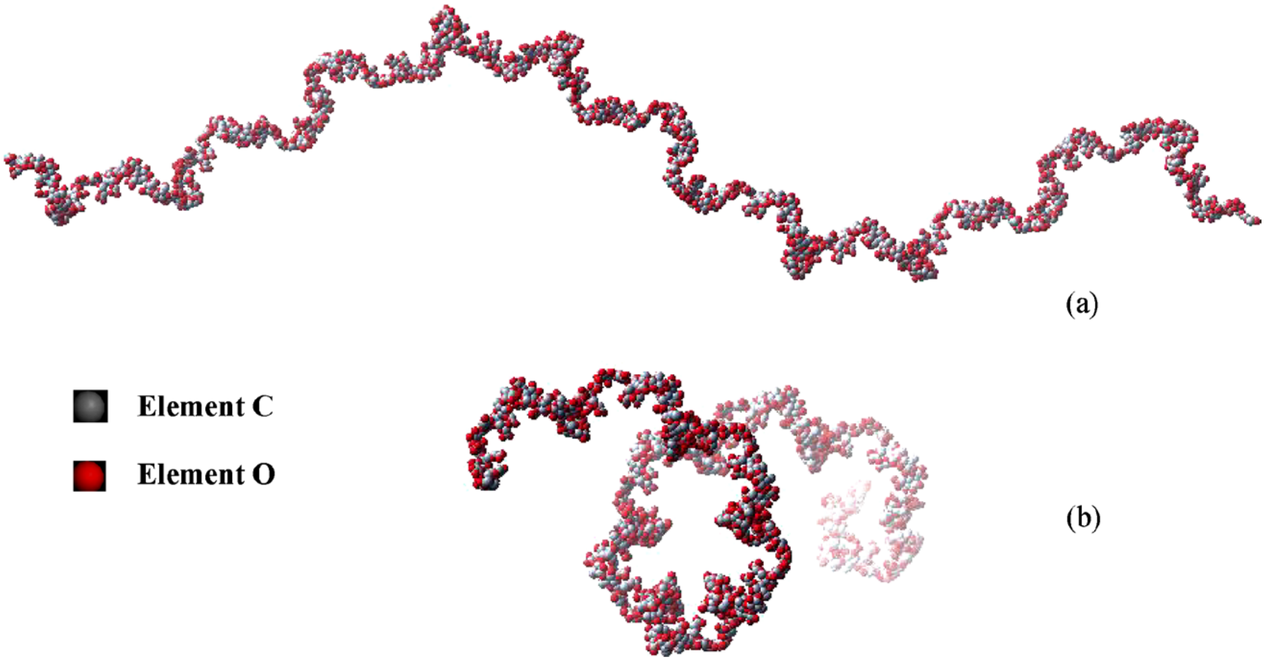

Fig. 3. Computer simulated (a) latitudinal view and (b) longitudinal view of molecular CPK (space filling) structure of CMC in aqueous environment (each contains 50 repeat units).

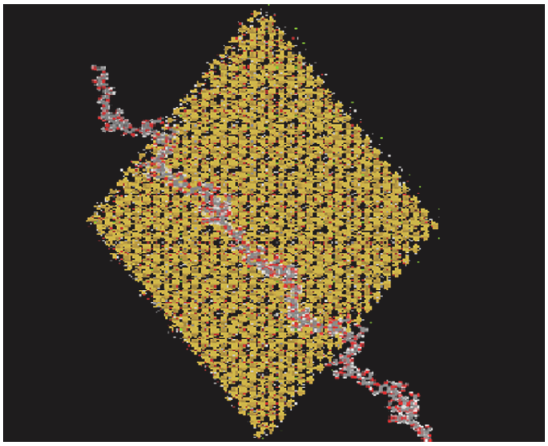

Fig. 4. Computer simulated structure of CMC molecule on talc surface.

of salt will reduce the electrostatic repulsion between them, which in turn will result in an increase of the CMC adsorption.

3.3.3. *Adsorption on talc with and without urea*

To explore the role of hydrogen bonding, adsorption tests were carried out in the presence of urea, a hydrogen bond breaker. Urea is a strong hydrogen bonding acceptor and it can be expected to affect the hydrogen bonding between the solid and the polymer in solution by preferential formation of hydrogen bonds between themselves and the polysaccharides and water. Adsorption isotherms of CMC on talc in the presence and absence of urea at pH 9 are shown in Fig. 8. It is clear that urea, the hydrogen bond breaker, reduces the adsorption of CMC on talc markedly. Therefore, it is proposed

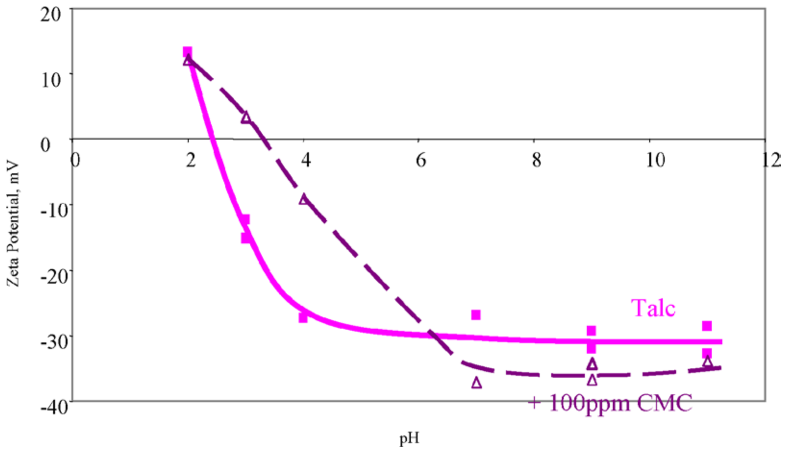

Fig. 5. Zeta potential of talc as a function of pH in the presence and absence of CMC.

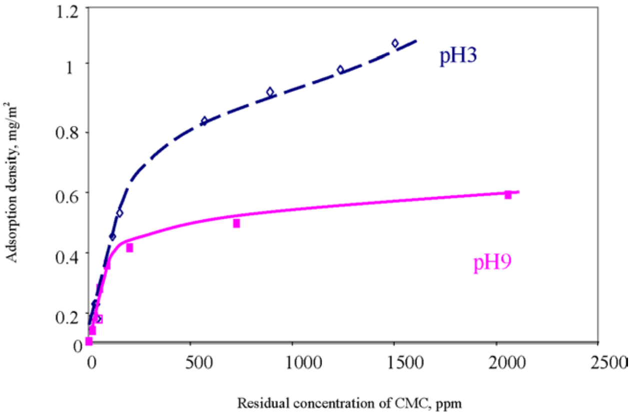

Fig. 6. Adsorption isotherm of CMC on talc at different pH.

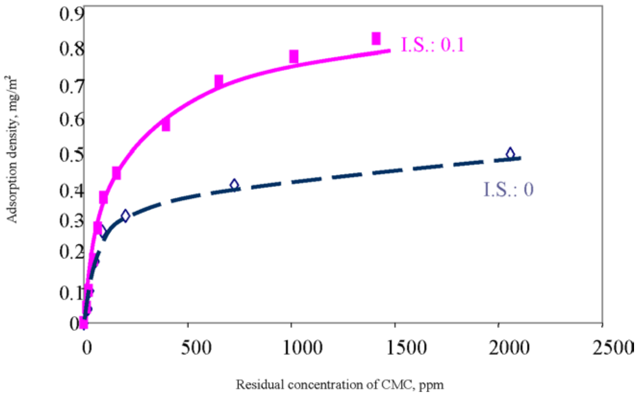

Fig. 7. Adsorption isotherm of CMC on talc at different ionic strength.

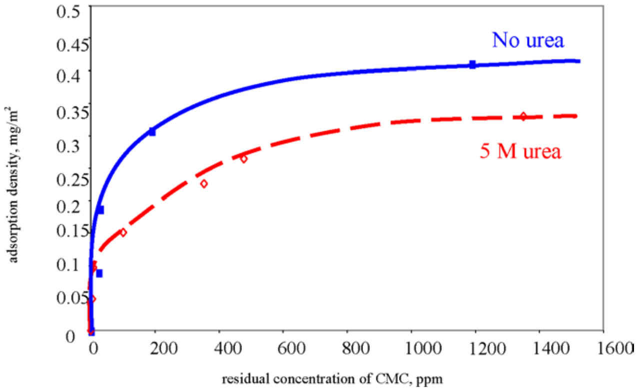

Fig. 8. Adsorption isotherms of CMC on talc with and without urea ($I = 0$, pH 9).

that hydrogen bonding plays a similar important role in the adsorption of CMC on talc.

Table 1
The calculated values of $(x/m)_{\max}$, ΔG^0_{ads} and σ^0 for the adsorption of CMC on talc at $T = 25\,^\circ\text{C}$

Polymer	$(x/m)_{\max}$ (mg/m^2)	ΔG^0_{ads} (kJ/mol)	σ^0 (nm^2)
CMC, pH 9	0.53	−22.3562	2146.6
CMC, pH 3	1.005	−21.0993	1150.2

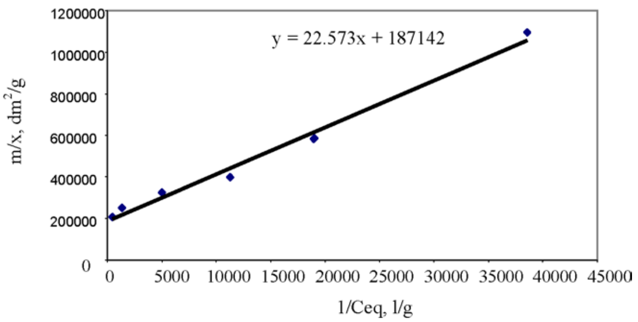

Fig. 9. Langmuir plot for adsorption of CMC on talc at pH 9, $T = 25\,^\circ\text{C}$.

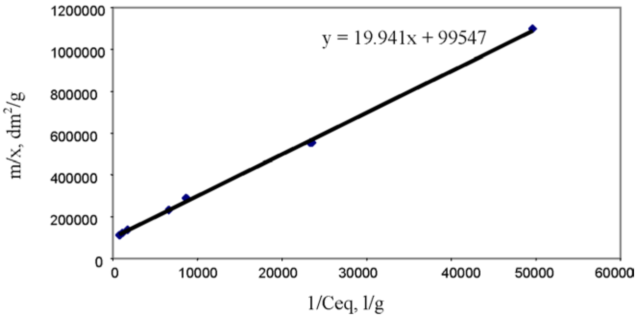

Fig. 10. Langmuir plot for adsorption of CMC on talc at pH 3, $T = 25\,^\circ\text{C}$.

3.3.4. *Modeling of polysaccharide adsorption on solid surface*

To obtain a better understanding of the adsorption mechanism of CMC on solids, the following parameters are extracted from the adsorption isotherms as shown in Table 1: standard free energy of adsorption ΔG^0_{ads}, maximum amount of polymer adsorbed per mass of solid, $(x/m)_{\max}$, and effective substrate area occupied per polymer chain, σ^0, at the talc/solution interface. The adsorption isotherms of CMC on solids measured in this study exhibited a pseudo-Langmuirian behavior. According to the Langmuir adsorption model applied to the polymer systems [17], surface coverage

$$\theta = KC/(1 + KC) = (x/m)/(x/m)_{\max}. \tag{1}$$

Equation (1) can be expressed as

$$m/x = 1/\left[K(x/m)_{\max}C_{\text{eq}}\right] + 1/(x/m)_{\max}, \tag{2}$$

where C_{eq} is the equilibrium solution concentration of polymer, x is the amount of polymer adsorbed, m is the mass of solid substrate, K is the Langmuir adsorption equilibrium constant and $(x/m)_{\max}$ is the maximum amount of polymer adsorbed per mass of solid. A plot of m/x against $1/C_{\text{eq}}$ should yield a linear relationship. The values of K and $(x/m)_{\max}$ can be determined from the intercept and slope of such a plot as shown in Figs. 9 and 10.

The Langmuir adsorption equilibrium constant, K, can be considered to represent the affinity of a polymer for a particular surface. It can be related to the standard free energy of adsorption, ΔG^0_{ads}, from the expression given in Eq. (3):

$$\Delta G^0_{\text{ads}} = -RT \ln K, \tag{3}$$

where R is the general gas constant ($R = 8.314\ \text{J}/(\text{mol K})$ and T is the absolute temperature.

From the maximum adsorption density, the effective area occupied on the substrate surface per polymer chain, σ^0, can be calculated using the following equation:

$$\sigma^0 = \theta \frac{A}{n_2^{\text{s}} N_{\text{A}}}, \tag{4}$$

where N_{A} is Avogadro number. θ is the fraction of the surface which is covered by polymer, A is the substrate surface area, and n_2^{s} is the number of moles of polymer adsorbed.

The number of moles of polymer adsorbed per unit area of solid, n_2^{s}/A, is given by Eq. (5):

$$\frac{n_2^{\text{s}}}{A} = \frac{(x/m)_{\max}}{M_{\text{w}}}, \tag{5}$$

where M_{w} is the molecular weight of the polymer. Hence, the effective substrate area occupied per polymer molecule, σ^0, can be calculated using Eq. (6):

$$\sigma^0 = \theta \frac{M_{\text{w}}}{(x/m)_{\max} N_{\text{A}}}. \tag{6}$$

From Table 1, it can be seen that ΔG^0_{ads}, calculated for CMC, indicates that adsorption of this polymer on talc is highly favored, i.e. $\Delta G^0_{\text{ads}} < 0$. It is apparent that the values of ΔG^0_{ads} are around -22 kJ/mol. As is well known, the free energy of hydrogen bond formation is about -25 kJ/mol, which is very close to the ΔG^0_{ads} of the polymer. Moreover, if hydrophobic interaction is the major force for adsorption, then a theoretical value around -50 kJ/mol might be expected for ΔG^0_{ads} [18], which is much greater than the calculated value. These results further confirm the major role of hydrogen bonding rather than hydrophobic force in governing CMC adsorption.

For a particular polymer, the value of σ^0 will be determined by the conformation that the polymer adopts upon adsorption. Clearly, σ^0 will be much greater if the polymer is adsorbed mainly in "trains" (a conformation in which the majority of the polymer is in contact with the surface) than if it adsorbs in the form of a high degree of "loops" and "tails" (one in which a lower proportion of the polymer segments are in contact with the surface). As shown in Table 1, the σ^0 of CMC are very high (very close to the molecular simulation results), which means that most segments of these polymers adsorb flat on talc. Since CMC is negatively charged at pH 9, σ^0 is larger than that at pH 3.

3.4. *FTIR spectroscopy*

Fig. 11 shows the IR spectrum of carboxymethyl cellulose. The band at 2924 cm^{-1} is due to C–H stretching of the –CH_2 groups. The band due to ring stretching of glucose appears at 1611 cm^{-1}. In addition, the bands in the region 1350–1450 cm^{-1} are due to symmetrical deformations of CH_2 and COH groups. The bands due to primary alcoholic –CH_2OH stretching mode and CH_2 twisting vibrations appear at 1078 and 1021 cm^{-1}, respectively. The weak bands at around 770 cm^{-1} are due to ring stretching and ring deformation of α-D-(1–4) and α-D-(1–6) linkages.

Fig. 12 shows the spectra of talc, CMC and CMC adsorbed talc. The FTIR spectrum of talc is shown in Fig. 12a. According to the characteristic IR frequencies of talc reported by other researchers [19], the band at around 1039 cm^{-1} can be assigned to the out-of-plane symmetric Si–O–Si mode. The Si–O bending vibration for talc has been observed at 432 cm^{-1} in the spectrum. The other bands in the spectrum around 654, 604, 550, 481 and 450 cm^{-1} are probably associated with various Mg–OH modes. The band at around 384 cm^{-1} appears to involve mixed vibrations of the Si–O network, the octahedral cations and the hydroxy groups. The band at 374 cm^{-1} is associated with the symmetric Mg–OH vibration. Talc also shows a single Mg–OH

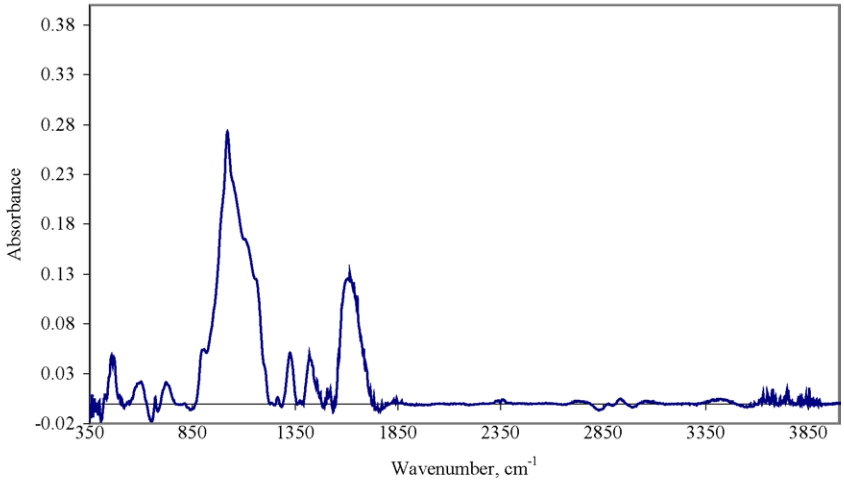

Fig. 11. FTIR spectrum of carboxymethyl cellulose.

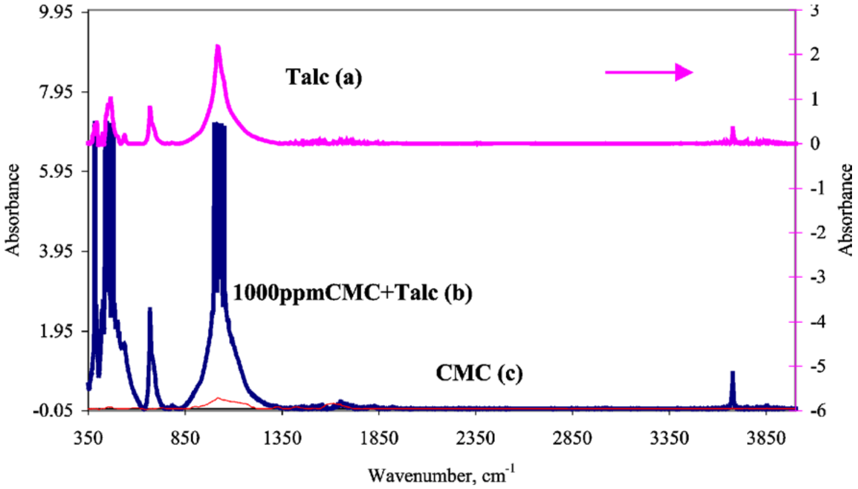

Fig. 12. FTIR spectra of talc, CMC and CMC adsorbed talc.

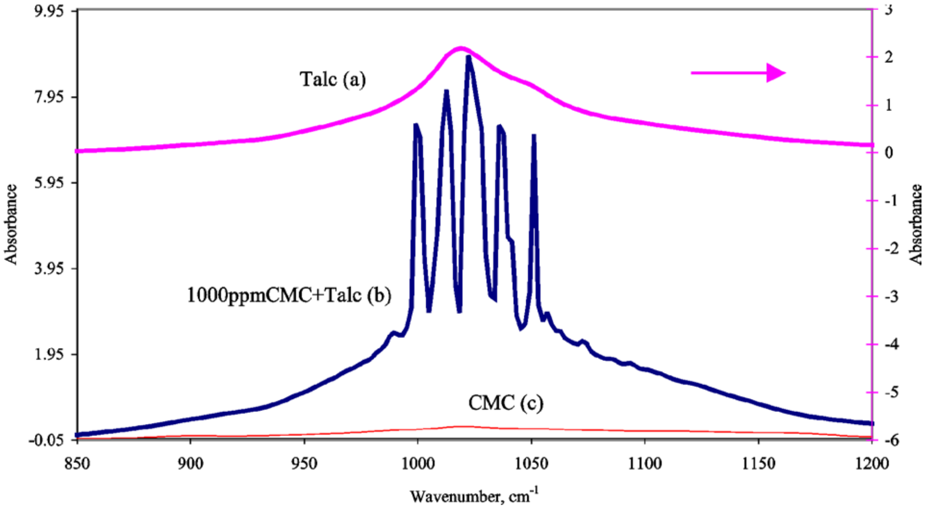

Fig. 13. FTIR spectra of talc, CMC and CMC adsorbed talc (850–1200 cm^{-1}).

stretching band around 3677 cm^{-1} due to the centrosymmetric relationship between the hydroxy groups on both sides of the octahedral layers.

From the spectrum of CMC adsorbed talc (Fig. 12b), the characteristic absorption peaks at 1642 cm^{-1} due to the carbonyl of the carboxyl groups of CMC appeared to be less sharp and shifted to 1680 cm^{-1} after adsorption. In addition, from Fig. 13, it is clear that the band at around 1039 cm^{-1} for the out-of-plane symmetric Si–O–Si mode is split into five sharp peaks and appear at around 1000–1080 cm^{-1} after CMC adsorption. The difference in IR spectrum is attributed to the hydrogen bonding formation between the primary alcoholic –CH_2OH and Si–O–Si after adsorption [20]. The changes in the infrared bands in the region 1000–1080 cm^{-1}, associated with the C–O stretch coupled to the C–C stretch and O–H deformation, were significant and therefore support strong hydrogen bonding of CMC to the solid surface. Strong hydrogen bonding would be expected to affect the C–O stretching. The decrease in the O–H stretching wavenumber of the primary alcoholic –CH_2OH from 1078 cm^{-1} to below 1050 cm^{-1} relative to the non-adsorbed polysaccharide suggests that the hydrogen bonds have become stronger upon adsorption. Hence, the CMC molecules appear to be more strongly hydrogen-bonded to the talc than they were to each other before adsorption.

3.5. *Fluorescence spectroscopy*

To better understand the nature of CMC adsorption, the microstructure of the adsorbed layer was probed using fluorescence spectroscopy. Fluorescence spectroscopy is a well-developed method [21] for monitoring hydrophobic domain formation due to adsorption. Fluorescence data for the pyrene labeled CMC adsorbed talc–solution interface is shown in Fig. 14. The polarity parameter decreases with the increase in concentration of CMC, suggesting no hydrophobic domain at the talc–aqueous interface; instead, the fluorescence results suggest formation of hydrophilic domains for the adsorption of CMC on talc.

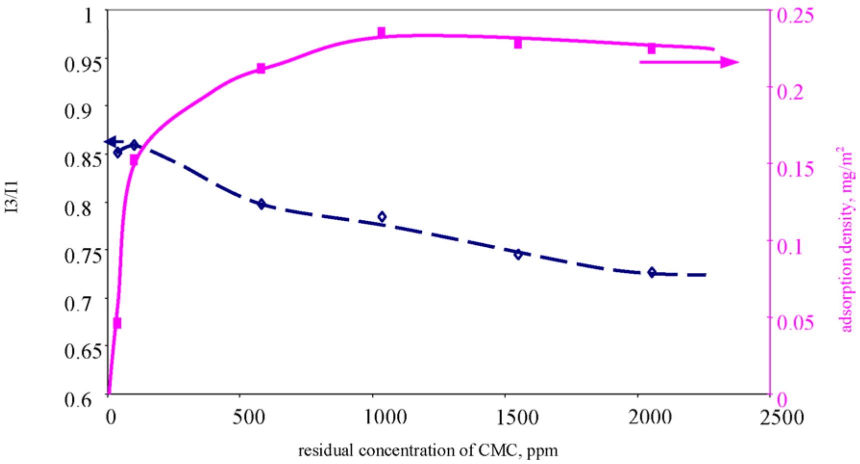

Fig. 14. Pyrene fluorescence for CMC and talc interface (pH 8.5, no salt).

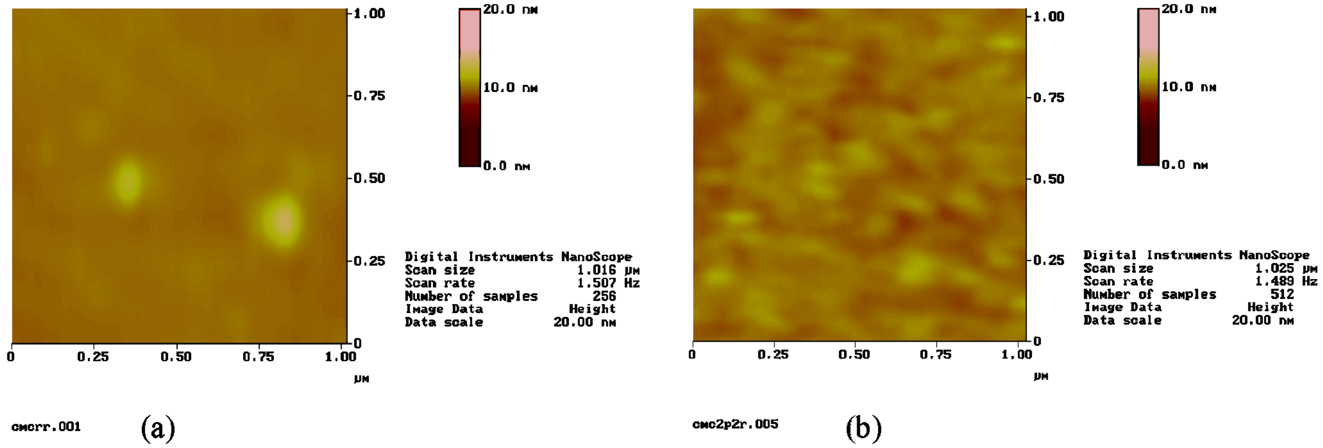

Fig. 15. AFM images of CMC adsorbed on mica at (a) pH 9, (b) pH 3 (C: 200 ppm).

3.6. *AFM analysis*

From AFM imaging [22–26] of CMC adsorbed mica surface (Fig. 15) at the same concentration of CMC (200 ppm), the surface of mica is more covered by CMC at pH 3 than at pH 9, which indicates that electrostatic interactions do affect CMC adsorption on solid. In addition, the average thickness of adsorbed clusters is around 1 nm, suggesting a flat conformation of this polymer on the solid surface.

4. Conclusions

(1) Electrokinetic studies of adsorption of carboxymethyl cellulose (CMC) on talc in the pH range of 2–11 showed the CMC to decrease negative zeta potential of talc with a shift of the iep from pH 2.5 to pH 3.5. In addition, the adsorption of CMC on talc was found to be affected by changes in pH and ionic strength. These results suggest that the electrostatic force plays an important role in the adsorption of CMC on talc.

(2) The FTIR results provide data on spectral changes that are associated with hydrogen bonding between polysaccharides and the solid surface. The changes in the infrared bands in the region of 1000–1080 cm^{-1}, associated with the C–O stretch coupled to the C–C stretch and O–H deformation, were significant and thus support strong hydrogen bonding of polysaccharides on the solid.

(3) Fluorescence tests gave no evidence for hydrophobic domain formation upon the adsorption of CMC at talc–aqueous interface, suggesting instead the governing role of hydrophilic forces.

(4) Urea, a hydrogen bond breaker, reduced the adsorption of CMC on talc significantly. This result also supports a mechanism involving hydrogen bonding rather than a hydrophobic one.

(5) From molecular modeling, a helical structure is observed for CMC in aqueous environment. The polymer was found to adsorb flat on the solid surface to let more of its OH groups to be in contact with the surface.

(6) Langmuir modeling of adsorption isotherm further supports the hydrogen bonding as the dominant force for polysaccharide adsorption since the adsorption free

energy of these polymers is close to that of hydrogen bond formation. Polysaccharides were also interpreted to adsorb in a very flat conformation according to the calculated effective area occupied on the substrate surface per polymer chain and AFM analysis.

Generally speaking, CMC adsorption on talc is dominated by both electrostatic interaction and hydrogen bonding. It is proposed that CMC adsorbs flat on solid surface to achieve maximum interaction between the hydroxyl groups on polymer chain and the solid surface sites.

Acknowledgments

The authors acknowledge the support of the National Science Foundation (Grant# CTS-00-89530 Dynamic Aggregation Behavior of Surfactant Mixture In Solutions at Solid/Liquid Interface) and Cytec Industries.

References

[1] J.M.W. Mackenzie, EGMJ (October 1980) 80–87.
[2] Z. Tian, Z. Wu, in: M.J. Jones, P. Gill (Eds.), Mineral Processing and Extractive Metallurgy, The Institute of Mining and Metallurgy, London, 1984, pp. 743–750.
[3] M.K. Rhodes, Proc. 13th International Mineral Processing Congress, Warsaw, 1979, pp. 346–366.
[4] E. Steenberg, P.J. Harris, S. Afr. J. Chem. 37 (1984) 85–90.
[5] R. Jin, W. Hu, S. Meng, Miner. Metall. Process. (1987) 227–232.
[6] M. Mackenzie, in: D. Malhotra, W.F. Riggs (Eds.), Chemical Reagents in the Mineral Processing Industry, Society of Mineral Engineerings, Colorado, USA, 1986, pp. 139–145.
[7] R.J. Pugh, Int. J. Miner. Process. 25 (1989) 101–130.
[8] T.W. Healy, J. Macromol. Sci. Chem. A 8 (1974) 603–619.
[9] R.K. Rath, S. Subramanian, Miner. Eng. 10 (1997) 1405–1420.
[10] R.K. Rath, S. Subramanian, J.S. Laskowski, Langmuir 13 (1997) 6260–6266.
[11] E. Steenberg, Ph.D. Thesis, Faculty of Science, University of Potchefstroom, Johannesburg, South Africa, 1982.
[12] E. Steenberg, P.J. Harris, S. Afr. J. Chem. 37 (1984) 85–90.
[13] P. Jenkins, J. Ralston, Colloids Surf. A 139 (1998) 27–40.
[14] R.K. Rath, S. Subramanian, J.S. Laskowski, in: J.S. Laskowski, G.W. Poling (Eds.), Processing of Hydrophobic Minerals and Fine Coal, Canadian Institute of Mining, Metallurgy and Petroleum, Montreal, Canada, 1995, p. 105.
[15] B.A. Jucker, H. Harms, S.J. Hug, A.J.B. Zehnder, Colloids Surf. B: Biointerfaces 9 (1997) 331–343.
[16] M. Dubois, K.A. Gilles, J.K. Hamilton, P.A. Rebers, F. Smith, Anal. Chem. 28 (1956) 350–356.
[17] D.J. Shaw, Introduction to Colloid and Surface Chemistry, Butterworth–Heinemann, Oxford, 1992.
[18] J.D. Miller, J.S. Laskowski, S.S. Chang, Colloids Surf. A 8 (1983) 137–151.
[19] J.T. Kloprogge, R.L. Frost, L. Rintoul, Phys. Chem. Chem. Phys. (1999) 2559–2564.
[20] P.K. Weissenborn, L.J. Warren, J.G. Dunn, Colloids Surf. A 99 (1995) 11–27.
[21] J.K. Thomas, The Chemistry of Excitation at Interfaces, Am. Chem. Society, Washington, DC, 1984.
[22] I. Capron, S. Alexandre, G. Müller, Polymer 39 (1998) 5725–5730.
[23] T.M. McIntire, R.M. Penner, D.A. Brant, Macromolecules 28 (1995) 6375–6377.
[24] A.P. Gunning, A.R. Kirby, M.J. Ridout, G.J. Brownsey, V.J. Morris, Macromolecules 29 (1996) 6791–6796.
[25] K.J. Wilkinson, E. Balnois, G.G. Leppard, J. Buffle, Colloids Surf. A 155 (1999) 287–310.
[26] R.K. Rath, S. Subramanian, Miner. Eng. 10 (12) (1997) 1405–1420.